J. Min. Metall. Sect. B-Metall. 58 (2) (2022) 335 - 344

Journal of Mining and Metallurgy, Section B: Metallurgy

EFFECT OF STRAIN ENERGY ON CORROSION BEHAVIOR OF ULTRAFINE GRAINED COPPER PREPARED BY SEVERE PLASTIC DEFORMATION

M. Rifai [a*], M. Mujamilah [b], E. Bagherpour [c], H. Miyamoto [d]

[a] Research Center for Accelerator Technology, Research Organization for Nuclear Energy, National Research and Innovation Agency, Serpong, Tangerang Selatan, Banten, Indonesia
[b] Research Center for Radiation Detector and Nuclear Analysis, Research Organization for Nuclear Energy, National Research and Innovation Agency, Serpong, Tangerang Selatan, Banten, Indonesia
[c] Brunel Center for Advanced Solidification Technology, Brunel University London, Uxbridge, UK
[d] Department of Mechanical Engineering, Doshisha University, Kyotanabe, Kyoto, Japan

(Received 01 January 2022; accepted 11 July 2022)

Abstract

Effect of strain energy on corrosion behavior of ultrafine-grained (UFG) copper prepared by severe plastic deformation (SPD) was investigated in terms of microstructural evolution. The SPD processed material showed an ultrafine-grained (UFG) structure after grain refinement for several time processes, which will affect mechanical and corrosion behavior Homogeneity can be obtained efficiently through the pressing process commonly known as simple shear extrusion (SSE), which is one of the SPD techniques. Pure copper was processed by SSE for two, four, eight, and twelve passes. The structure of SSE treated sample was observed by laser microscope and transmission electron microscope as well as X-ray diffraction. The corrosion behavior by potentiodynamic polarization curve was observed in modified Livingstone solution, 1 M NaCl, and sulphuric solution. The structure of SSE processed sample showed that the first pass of the SSE processed sample displayed large deformation by developing the elongated grain and sub-grain structure. By increasing the SSE pass number, the grain shape became equiaxed due to excessive strain. The X-ray broadening related to ultrafine-grained (UFG) structure processed SSE on the copper sample, leading to smaller crystallite size, higher microstrain, and higher dislocation density. More homogeneous passive film was developed on the material with UFG structure appearance. However, the current density in 1 M NaCl was decreased by an increment of pass number due to the dissolution of copper metal. The UFG structure has more boundaries than coarse grain structure, and these phenomena show why Cu dissolve ability influences the current density. The grain boundary behaves as the cathodic site.

Keywords: *Plastic deformation; Energy strain; Ultrafine grain structure; Grain boundary*

1. Introduction

Severe plastic deformation (SPD) has been used to improve material properties by modifying its structure [1, 2]. The SPD structure has a unique characteristic due to high deformation level [3], grain shape [4], and dislocation density [5]. The SPD processed material showed an ultrafine-grained (UFG) structure after grain refinement for several time processes, which affect mechanical and corrosion behaviour, such as corrosion stress cracking [6, 7], fatigue corrosion [8], anodic polarization [9], and tafel corrosion test [10]. Corrosion behavior of UFG material has not been appropriately investigated due to the lack of understanding of this unique UFG material.

Previous studies have shown that the UFG microstructure in copper, which is relatively homogeneous, can be obtained efficiently through the pressing process commonly known as simple shear extrusion (SSE) [11]. The final grain sizes obtained by the SSE method were comparable to those obtained by the equal channel angular pressing (ECAP) method. SSE method has simple channel extrusion, which is less complicated and easier than the ECAP technique due to slight rotation inside the SSE die [11]. The advantages of the SSE method over other processes are that it is inexpensive and straightforward, and also can carry out mass production of sheet metal continuously and has excellent potential for commercialization [11].

The effect of grain refinement on corrosion behavior can be exemplified by copper metallic material due to its convenience and soft material to be processed by SSE. The copper also has a suitable

* *Corresponding author: iamrifai@yahoo.com*

https://doi.org/10.2298/JMMB220101015R

property for conductivity and virus inactivation. This characteristic may be enhanced by the SSE process. The previous report mentioned that the corrosion resistance of UFG copper had been improved due to nanostructure conditions [7]. This research aims to observe the structure evolution by severe plastic deformation and investigate the effect of dislocation density on corrosion resistance in several solutions.

2. Experimental procedure

The material that was treated in this study is 99.9% copper by Nilaco, Japan. The sample was cut from the ingot,twenty 10 mm x 10 mm billets. The billets were annealed at 673 K for two hours. The billets were processed by simple shear extrusion for two, four, eight, and twelve passes repeatedly in Autograph Shimadzu 500 kN at room temperature. The extrusion was done by SSE die with 23.6° angles in one line extrusion method which is equal to 1.15 equivalent strains (3D concept direction as seen in Figure 1). Due to high friction between the die and the billet, MoS_2 lubricant needs to be applied on the billet. The billet was cut for the transverse plane, grounded, and polished until it got a smooth surface for structure observation and corrosion testing. The structure observation was carried by a scanning electron microscope JEOL 7001F FE-SEM and transmission electron microscope (TEM) JEOL 2100F. The diffraction pattern of metallic material was measured by X-ray Diffraction (XRD) Rigaku SmartLab with scan angle 2 θ, 30°-80°. The corrosion behaviour was investigated by potentiodynamic polarization curve in several solutions like the modified Livingston etchant, NaCl, and H_2SO_4 at room temperature. Reference electrode Ag/AgCl and platina electrode were used in this corrosion testing as standard corrosion testing. The corroded surface was observed by a laser microscope Keyence 3D Laser Scanning Microscope – VK-X100.

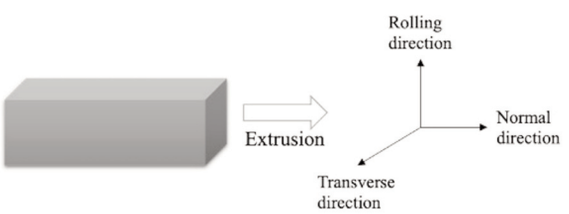

Figure 1. *The schema of SSE billet in term of deformation plane*

3. Results

3.1. Microstructural Characterization

The structure of as-annealed copper observed by an optical microscope exhibited an average of 25 μm grain size, as seen in Figure 2. The as-annealed sample showed homogeneous [12] and coarse grain structure [13] due to the heat-treatment process at 673 K for two hours [14]. Figure 3 shows the microstructure of as annealed and as SSE processed material up to twelve passes. The micrograph was taken by electron backscattered diffraction (EBSD) image pattern at the FE-SEM system. The grain size of copper material was decreased by increasing the SSE processed pass number. The first pass of the SSE process showed large deformation by developing the elongated grain and sub-grain structure. By increasing the SSE pass number, the grain shape became equiaxed due to excessive strain.

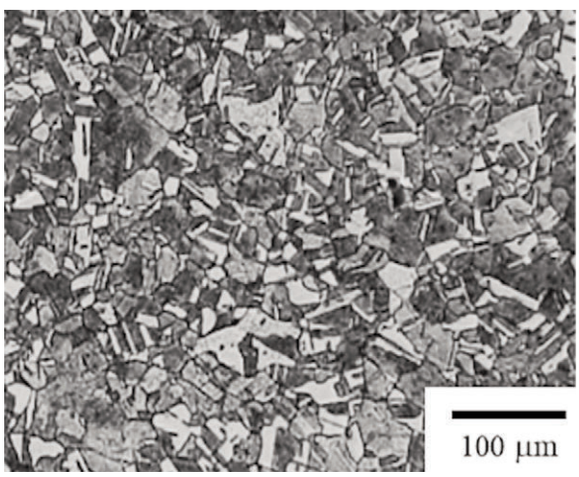

Figure 2. *Micrograph of the as-annealed copper sample*

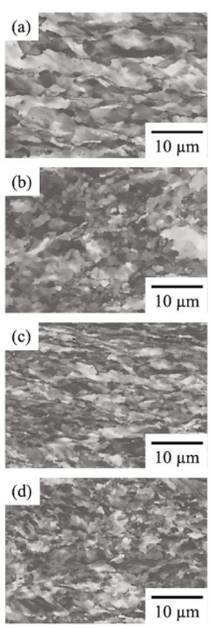

Figure 3. *Elongated grain and sub-grain structure at the sample for (a) two; (b) four (c) eight; and (d) twelve SSE passes*

The large deformation on copper metallic material could influence the dislocation density, as confirmed by the red arrow at the TEM micrograph in Figure 4. After two passes, one grain showed high dislocation density in the grain boundary area (pointed by red arrow), indicating the SSE process was sufficient to promote dislocation appearance in copper material.

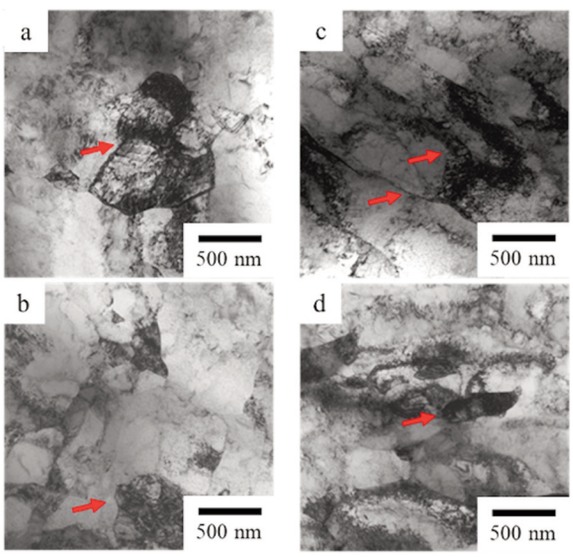

Figure 4. *Transmission electron microscope of (a) two SSE passes, (b) four, (c) eight, and (d) twelve SSE passes. After two passes, one grain showed high dislocation density in the grain boundary area (pointed by red arrow), indicating the SSE process was sufficient to promote dislocation*

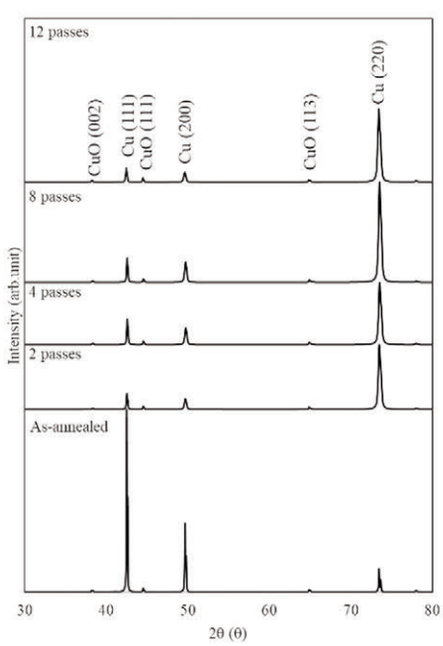

Figure 5. *X-ray diffraction (JCPDS 01-077-0199) of as annealed, two, four, eight, and twelve SSE passes*

Eight passes of the SSE processed sample showed higher dislocation density inside the grains than four passes due to excessive deformation on the rolling direction [15]. However, after twelve passes, the structure became homogeneous and had lower dislocation density than eight passes, even though several elongated grains still could be seen in the micrograph. During the SSE process, the dynamic recovery and recrystallization may occur due to the warm process and excessive forming due to the appearance equilibrium grain boundary after twelve passes of SSE.

Figure 6 shows the X-ray diffraction pattern for an annealed and SSE processed sample. As-annealed sample exhibited Bragg reflection on Cu with (111); (200); (220) plane, and CuO with (002). (111), and (113). This diffraction pattern was extracted the full width half maximum (FWHM) value relevant to crystallite size, microstrain, and dislocation density. The dislocation density can be measured by the Williamson-Hall Method (broadening of XRD pattern). After four passes and eight passes, the

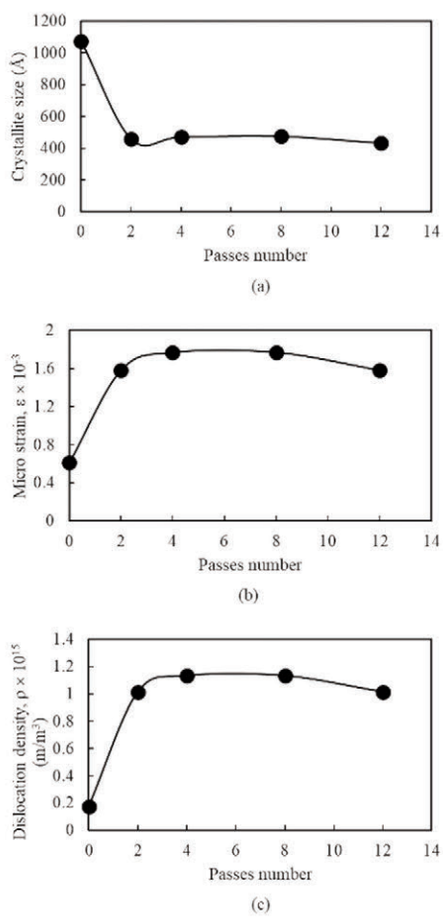

Figure 6. *The data analyzed from XRD data, such as crystallite size, microstrain, and dislocation density*

FWHM showed larger broadening than two passes and an as-annealed sample as a coarse grain structure. This broadening related to ultrafine-grained (UFG) structure processed SSE on the copper sample, leading to smaller crystallite size, higher microstrain, and higher dislocation density, as seen in Figure 6. SSE process promotes larger defects on the material, which increase the microstrain and dislocation density due to large deformation value. The dislocation density can be confirmed by the TEM micrograph in Figure 4, in which the highest dislocation can be reached at eight SSE passes. This dislocation density of eight passes can be related to dislocation stacking in the copper material slip plane as a face-centred cubic system. However, twelve passes showed a decrement on FWHM. The twelve SSE passes show that the dislocation density decreased due to the annihilation process by dynamic recovery and recrystallization during the deformation process.

3.2. Corrosion behavior

The corrosion behavior of the as-annealed and SSE processes sample was investigated by electrochemical testing in several solutions. Figure 7 shows the potentiodynamic polarization curve in modified Livingstone etchant and 1 M NaCl, which can be extracted from the value of potential corrosion and current density in terms of pass number (equivalent strain) and grain size, in Figure 8 and 9, respectively. The corrosion potential is associated with the corrosion resistance characteristic of the material, whereas the corrosion density is associated with the corrosion rate of the material. The potential corrosion and current density of the material in modified Livingstone etchant increase by incrementing pass number due to the passive form of UFG structure. This result was confirmed by a previous result that mentions the transition of corrosion type [11]. More homogeneous passive film was developed on the material with UFG structure appearance. A similar manner also happened in 1 M NaCl. However, the current density in 1 M NaCl was decreased by an increment of pass number due to the dissolution of copper metal. The UFG structure has more boundaries than coarse grain structure, and these phenomena show why Cu dissolve ability influences the current density. The grain boundary behaves as the cathodic site. This occurrence also can be seen in terms of grain size in Figure 9.

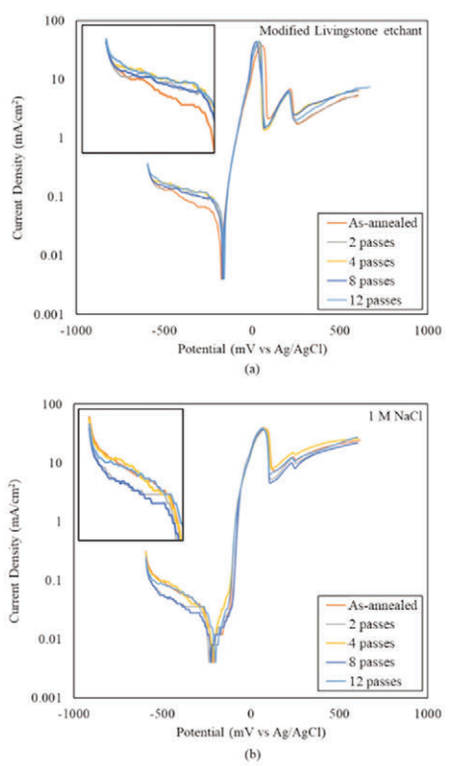

Figure 7. *Potentiodynamic polarization curves of copper SSE processed sample in (a) modified Livingston etchant and (b) 1 M NaCl*

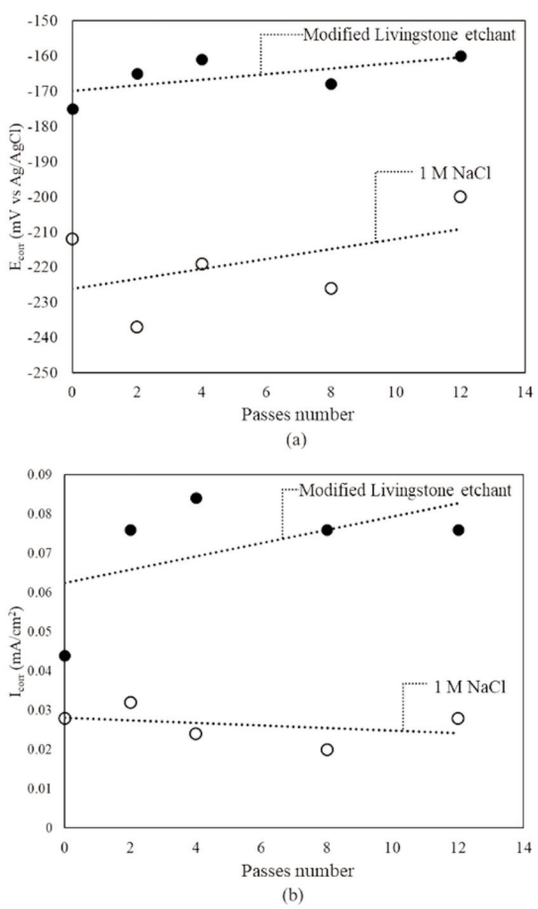

Figure 8. *Effect of copper SSE passes number on (a) corrosion potential, and (b) current density in modified Livingston etchant*

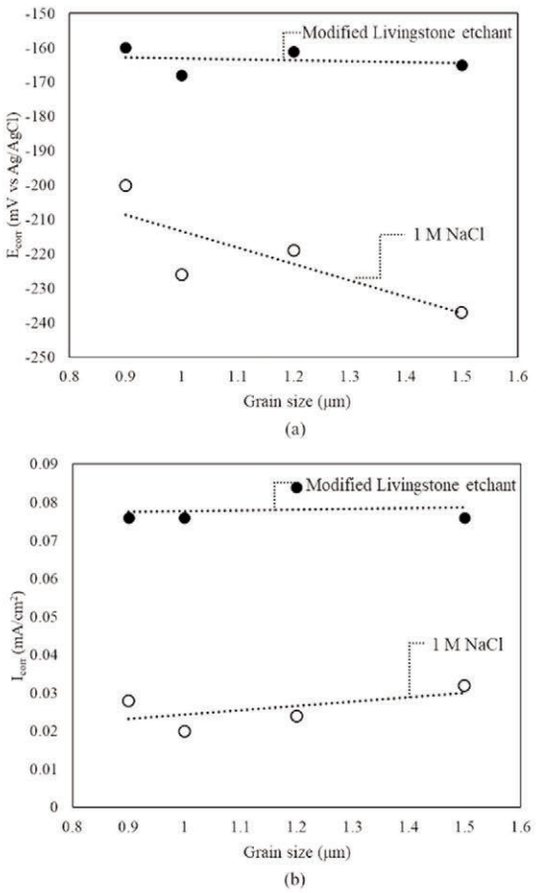

Figure 9. *Effect of grain size on (a) corrosion potential, and (b) current density in modified Livingston etchant*

Figure 10 shows the corrosion behavior related to the active-passive transpassive curve of copper metal between 100-400 mV vs Ag/AgCl, of Ep1; the first passive film was related to Cu_2O formation, and the second passive film was associated with CuO in modified Livingston etchant and 1 M NaCl, respectively. Both passive films could be a mixture due to the high potential in the electrochemical test, which was related to passive film of copper metal-the sweep rate of corrosion testing effects to active-passive transition, as seen in Figures 11 and 12. The grain size influence can be seen in the first passive layer of copper metal; it means the passivation of UFG material is more accessible to form than as-annealed material. The transition corrosion type was occurred after the SSE process due to passivity in neutral solution [11].

The second passive layer showed a similar appearance between as annealed and SSE processed sample in modified Livingston etchant solution as shown in Figure 11. It indicated that the corrosion reaction to form CuO and Cu_2O was similar between UFG and coarse grain structure. The CuO and Cu_2O formation can be explained by the dissolution at acidic and alkali solutions [18]. This second passive was also associated with the crystalline structure due to the high diffusion rate of UFG material on the surface area. The diffusion process on the UFG structure occurred faster so that the ions could be easily carried into the surface, hence adequately improving the corrosion resistance. The cupric ions in the UFG material surface were more straightforward to diffuse than in the coarse grain structure. This phenomenon took place also in the grain interior, leading to higher corrosion resistance, as seen in the cathodic reaction in Figure 6. It could also be observed from intergranular corrosion on the material surface, as seen in Figure 12. This corroded surface

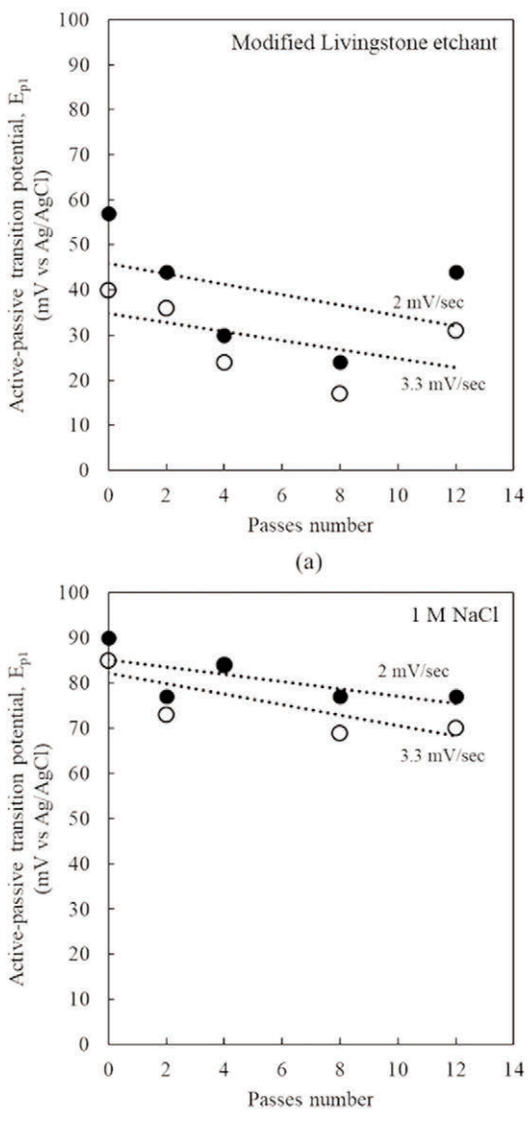

Figure 10. *Effect of copper SSE passes number on Active-passive transition potential, Ep1 in (a) Modified Livingston etchant and (b) 1M NaCl solution*

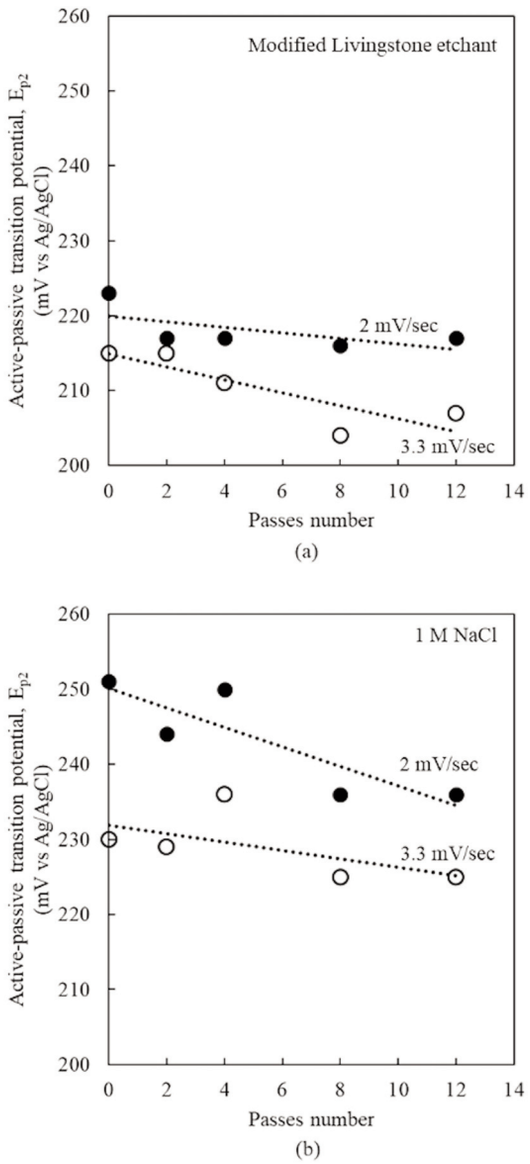

Figure 11. *Effect of copper SSE passes number on Active-passive transition potential, Ep2 in (a) Modified Livingston etchant and (b) 1M NaCl solution*

also can be confirmed by other SPD techniques, like ECAP, that mentioned corrosion transition during the grain refinement process [18]. It is inferred that the increasing pass number leads to higher corrosion resistance due to the passive film formation on the copper sample.

The corroded surface observed by a laser microscope was used to investigate the damage level after corrosion testing, as seen in Figure 12. The corrosion behavior of the SSE processed sample by H_2SO_4 solution was carried out at anodic polarization because the SSE processed sample shows a significant change in terms of microstructure evolution and grain refinement. This corrosion appearance could be

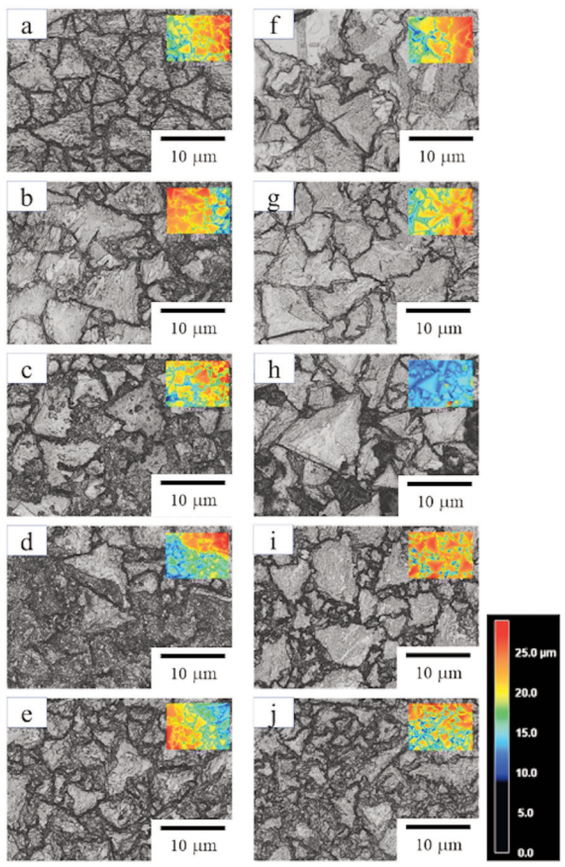

Figure 12. *Corrosion appearance of copper SSE processed sample in modified Livingston etchant by laser microscope for (a) as-annealed, (b) two, (c) four, (d) eight, (e) twelve, and in 1 M NaCl for (f) as-annealed, (g) two, (h) four, (i) eight, and (j) twelve*

related to structural homogeneity after the SSE process, which exhibited intergranular corrosion due to a higher fraction of grain boundaries. Because of a high corrosion rate in the copper sample, it was challenging to identify the corrosion sites, whether the

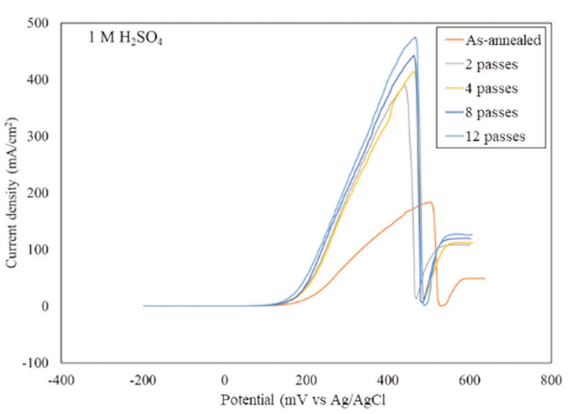

Figure 13. *Anodic polarization of copper SSE processed sample in 1M H_2SO_4*

grain boundary or materials matrix. The modified Livingston etchant (Figure 12.a - e) showed more intense corrosion than 1 M NaCl solution (Figure 12.f - j) on the copper surface, indicated by the deep grooves on the surface. The intensity color explains the corrosion level in each material, and it shows that the annealed and low pass number of the SSE process shows a high fraction in the red area. By increasing the pass number, the corrosion level becomes homogeneous due to the UFG structure. The final corrosion test solution was sulphuric acid, which can also investigate the corrosion resistance of copper material, as seen in Figure 13. The SSE processed sample showed a high dissolution rate in sulphuric acid compared to other solutions.

4. Discussion

The grain refinement by the SSE process can be used to improve the mechanical properties and corrosion resistance. The SSE process's corrosion resistance mechanism on the UFG structure needs to be elaborated in more detail by potentiodynamic measurement [16-20]. The potentiodynamic polarization curve showed constant cathodic currents and higher anodic currents due to the grain refining process. The potentiodynamic polarization curve of the UFG structure moved to a higher value compared to the coarse grain structure, meaning that corrosion resistance improved significantly. The anodic currents associated with corrosion currents indicated the weight loss of material; in this case, the UFG structure showed lower weight loss than coarse grain structure due to high dislocation density and a high fraction of grain boundaries. This phenomenon also appeared in the ECAP process, and their results mentioned that the high fraction grain boundaries corroded faster than coarse grain [18]. The corrosion speed was also associated with corrosion current, determined by anodic and cathodic reactions. The grain boundaries showed a higher dissolution rate than inside grain due to activation energy for active formation [18]. The grain boundaries and the grain interior showed the appearance of local micro cells after the deformation process, and it can be seen in cathode sites [18]. The UFG structure also might be more active than the coarse grain structure due to extra free energy [18, 21,25]. Grain refinement influenced the corrosion current density due to a lower cathodic area related to grain interior; as seen in Figure 14; it may explain the corrosion behavior of pure copper UFG structure. The grain boundaries showed a lower dissolution rate than the grain interior, so that the UFG structure may perform better corrosion behavior. In other words, the grain refinement promotes the corrosion current corresponding to the dissolution rate.

SSE processed sample at eight passes represented

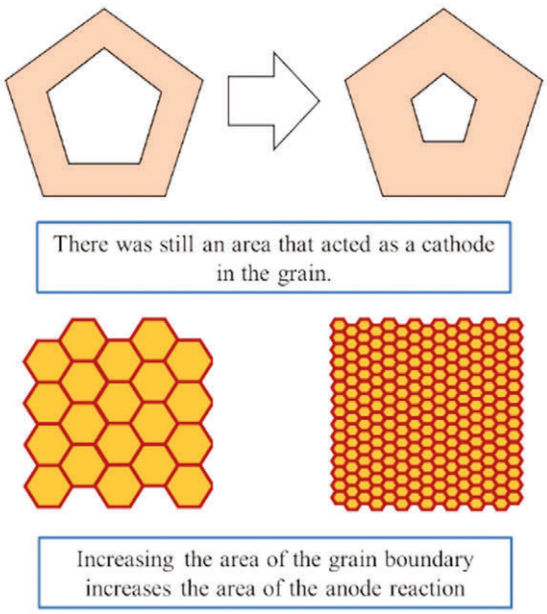

Figure 14. *Anodic polarization of copper SSE processed sample shows the change in the cathode. However, the anode appearance remained constant due to the increasing grain boundary area*

a non-equilibrium grain boundary state, having higher dislocation density than coarse grain material. It may promote the activation energy associated with the dissolution process [21-25]. After twelve passes, the non-equilibrium grain boundaries transformed into equilibrium grain boundaries due to large deformation. On the one hand, the corrosion appearance of the SSE processed sample showed homogeneous corrosion sites along grain boundaries. On the other hand, as annealed or coarse grain samples showed localized damage. The corrosion sites of the UFG structure may affect the formation of the uniform passive layer because of the grain refinement in the UFG structure. Previous studies mentioned that higher corrosion resistance of UFG structure material might associate with impurities segregation at grain boundaries and promote a higher passivation rate [26, 27], and it also occurred in iron chromium alloy as pure crystal structure metallic material [28-32]. This occurrence showed an intergranular attack at grain boundaries. The main parameter affecting corrosion behavior was dislocation and grain boundaries since they showed the intrinsic attack at local sites and high free energy. Finally, the homogeneity of UFG structure with equilibrium grain boundaries may control the corrosion behavior and the effect of ratio anode-cathode area to weight loss from potentiodynamic polarization curve by UFG structure and equilibrium grain boundaries state.

5. Conclusion

Severe plastic deformation affects strain energy and corrosion behavior of UFG copper prepared concerning grain size. SSE processed samples exhibited small grain size with high dislocation density and high grain boundaries fraction due to significant deformation levels. After two passes, one grain showed high dislocation density in the grain boundary area, indicating the SSE process was sufficient to promote dislocation appearance in copper material. Eight passes of the SSE processed sample showed higher dislocation density inside the grains than four passes due to excessive deformation on the rolling direction. However, after twelve passes, the structure became homogeneous and had lower dislocation density than eight passes, even though several elongated grains still could be seen in the micrograph. During the SSE process, the dynamic recovery and recrystallization may occur due to the warm process and excessive forming due to the appearance equilibrium grain boundary after twelve passes of SSE.

The potentiodynamic polarization curves were used to explain the corrosion behavior of the UFG copper sample. This corrosion appearance could be related to structural homogeneity after the SSE process, which exhibited intergranular corrosion due to a higher fraction of grain boundaries. Because of a high corrosion rate in the copper sample, it was challenging to identify the corrosion sites, whether the grain boundary or materials matrix. The modified Livingston etchant showed more intense corrosion than 1 M NaCl solution on the copper surface, indicated by the deep grooves on the surface. The intensity color explains the corrosion level in each material, and it shows that the annealed and low pass number of the SSE process shows a high fraction in the red area. By increasing the pass number, the corrosion level becomes homogeneous due to the UFG structure. The final corrosion test solution was sulphuric acid, which can also investigate the corrosion resistance of copper material. The SSE processed sample showed a high dissolution rate in sulphuric acid compared to other solutions.

Acknowledgements

The authors gratefully acknowledge the financial support of a Grant-in-Aid for Scientific Research on Innovative Areas "Bulk nano metals," MEXT Japan (No 25102710) and Research and Innovation for Indonesia Research Fund Program (RIIM) No. B-811/II.7.5/FR/6/2022 and B-2103/III.2/HK.04.03/7/2022.

Author's contributions

In this paper, each author has different contributions, jointly designed and participated in the research process, obtained the data through synthesize, characterization, data analysis and finally there is no conflict of interest. The author's contributions are as follows: Muhammad Rifai carried out the experiment. Muhammad Rifai and Mujamilah wrote the manuscript with support from Hiroyuki Miyamoto. Muhammad Rifai and Ebad Bagherpour fabricated the SSE copper processed sample. Ebad Bagherpour and Hiroyuki Miyamoto helped supervise the project. Muhammad Rifai and Ebad Bagherpour conceived the original idea. Hiroyuki Miyamoto supervised the project.

Conflict of interest statement

We declare that all authors have no conflict of interest.

Data Availability Statement

The processed data needed to reproduce these findings cannot be shared at this time, as they also form part of an ongoing study, in accordance with the funder's data retention policy.

References

[1] J. Li, F. Li, C. Zhao, H. Chen, X. Ma, J. Li, Experimental study on pure copper subjected to different severe plastic deformation modes, Materials Science and Engineering: A, 656 (2016) 142-150. https://doi.org/10.1016/j.msea.2016.01.018

[2] A. Torkestani, M. R. Dashtbayazi, A new method for severe plastic deformation of the copper sheets, Materials Science and Engineering: A, 737 (2018) 236-44. https://doi.org/10.1016/j.msea.2018.09.054

[3] A. I. Rudskoi, A. M. Zolotov, R. A. Parshikov, Severe plastic deformation influence on engineering plasticity of copper, Materials Physics and Mechanics, 38 (1) (2018) 64-8. https://doi.org/10.18720/MPM.3812018_9

[4] M. Y. Alawadhi, S. Sabbaghianrad, Y. Huang, T. G. Langdon, Direct influence of recovery behaviour on mechanical properties in oxygen-free copper processed using different SPD techniques: HPT and ECAP, Journal of Materials Research and Technology, 6 (4) (2017) 369-377. https://doi.org/10.1016/j.jmrt.2017.05.005

[5] T. G. Sousa, V. L. Sordi, L. P. Brandão, Dislocation density and texture in copper deformed by cold rolling and ECAP, Materials Research, 21 (1) (2018). http://dx.doi.org/10.1590/1980-5373-MR-2017-0515

[6] T. Guo, S. Wei, C. Wang, Q. Li, Z. Jia, Texture evolution and strengthening mechanism of single crystal copper during ECAP, Materials Science and Engineering: A, 759 (2019) 97-104. https://doi.org/10.1016/j.msea.2019.05.042

[7] M. Lipińska, L. Olejnik, M. Lewandowska, The influence of an ECAP-based deformation process on the microstructure and properties of electrolytic tough pitch copper, Journal of Materials Science, 53 (5)

(2018) 3862-3875.
https://doi.org/10.1007/s10853-017-1814-y

[8] Z. N. Mao, R. C. Gu, F. Liu, Y. Liu, X. Z. Liao, J. T. Wang, Effect of equal channel angular pressing on the thermal-annealing-induced microstructure and texture evolution of cold-rolled copper, Materials Science and Engineering: A, 674 (2016) 186-192. https://doi.org/10.1016/j.msea.2016.07.050

[9] J. Xu, J. Li, D. Shan, B. Guo, Microstructural evolution and micro/meso-deformation behavior in pure copper processed by equal-channel angular pressing, Materials Science and Engineering: A, 664 (2016) 114-125. https://doi.org/10.1016/j.msea.2016.03.016

[10] M. Krystian, J. Horky, D. Colas, S. Neodo, F. Diologent, Microstructure, mechanical properties, and thermal stability of lean, copper-free silver alloy subjected to equal channel angular pressing (ECAP) and subsequent post-processing, Materials Science and Engineering: A, 757 (2019) 52-61. https://doi.org/10.1016/j.msea.2019.04.052

[11] E. Bagherpour, F. Qods, R. Ebrahimi, H. Miyamoto, Strain reversal in simple shear extrusion (SSE) processing: microstructure investigations and mechanical properties, AIP Conference Proceedings, 1920 (1) (2018) 020007. https://doi.org/10.1063/1.5018939

[12] J. Lu, X. Wu, Z. Liu, X. Chen, B. Xu, Z. Wu, S. Ruan, Microstructure and mechanical properties of ultrafine-grained copper produced using intermittent ultrasonic-assisted equal-channel angular pressing, Metallurgical and Materials Transactions A, 47 (9) (2016) 4648-4658. https://doi.org/10.1007/s11661-016-3622-4

[13] Y. Jiang, R. Zhu, J. T. Wang, Z. S. You, An investigation on rolling texture transition in copper preprocessed by equal channel angular pressing, Journal of Materials Science, 51 (12) (2016) 5609-5624. https://doi.org/10.1007/s10853-016-9862-2

[14] D. Gholami, O. Imantalab, M. Naseri, S. Vafaeian, A. Fattah-Alhosseini, Assessment of microstructural and electrochemical behavior of severely deformed pure copper through equal channel angular pressing, Journal of Alloys and Compound, 723 (2017) 856-685. https://doi.org/10.1016/j.jallcom.2017.06.302

[15] S. Kadiyan, B. S. Dehiya, Effects of severe plastic deformation by ECAP on the microstructure and mechanical properties of a commercial copper alloy, Materials Research Express, 6 (11) (2019) 116570. https://doi.org/10.1088/2053-1591/ab4a44

[16] M. Gholami, M. Mhaede, F. Pastorek, I. Altenberger, B. Hadzima, M. Wollmann, L. Wagner, Corrosion Behavior and Mechanical Properties of Ultrafine-Grained Pure Copper with Potential as a Biomaterial, Advanced Engineering Materials, 18 (4) (2016) 615-623. https://doi.org/10.1002/adem.201500269

[17] D. Yang, Y. Dong, H. Chang, I. Alexandrov, F. Li, J. Wang, Z. Dan, Corrosion behavior of ultrafine-grained copper processed by equal channel angular pressing in simulated sea water, Materials and Corrosion, 69 (10) (2018) 1455-1461. https://doi.org/10.1002/maco.201810165

[18] H. Miyamoto, Corrosion of ultrafine grained materials by severe plastic deformation, an overview, Materials Transactions, 57 (5) (2016) 559-72. https://doi.org/10.2320/matertrans.M2015452

[19] A. Fattah-Alhosseini, O. Imantalab, Y. Mazaheri, M. K. Keshavarz, Microstructural evolution, mechanical properties, and strain hardening behavior of ultrafine grained commercial pure copper during the accumulative roll bonding process, Materials Science and Engineering: A, 650 (2016) 8-14. https://doi.org/10.1016/j.msea.2015.10.043

[20] A. Fattah-Alhosseini, O. Imantalab, F. R. Attarzadeh. Enhancing the Electrochemical behavior of pure copper by cyclic potentiodynamic passivation: a comparison between coarse-and nano-grained pure copper, Metallurgical and Materials Transactions B, 47 (5) (2016) 2761-2770. https://doi.org/10.1007/s11663-016-0755-1

[21] A. Fattah-Alhosseini, O. Imantalab, Passivation behavior of ultrafine-grained pure copper fabricated by accumulative roll bonding (ARB) process, Metallurgical and Materials Transactions A, 47 (1) (2016) 572-580. https://doi.org/10.1007/s11661-015-3239-z

[22] W. Luo, L. Hu, Y. Xv, J. Zhou, W. Xv, M. Yan, Electrochemical corrosion behavior and surface passivation of bulk nanocrystalline copper in alkaline solution, Anti-Corrosion Methods and Materials, 67 (5) (2020) 465-472. https://doi.org/10.1108/ACMM-05-2020-2306

[23] O. M. Irfan, S. Mukras, F. A. Al-Mufadi, F. Djavanroodi. Surface Modelling of Nanostructured Copper Subjected to Erosion-Corrosion, Metals, 7 (5) (2017) 155. https://doi.org/10.3390/met7050155

[24] M. B. Mihajlović, M. B. Radovanović, A. T. Simonović, Ž. Z. Tasić, M. M. Antonijević, Evaluation of purine based compounds as the inhibitors of copper corrosion in simulated body fluid, Results in Physics, 14 (2019) 102357. https://doi.org/10.1016/j.rinp.2019.102357

[25] M. Naseri, D. Gholami, O. Imantalab, F. R. Attarzadeh, A. Fattah-Alhosseini, Effect of grain refinement on mechanical and electrochemical properties of severely deformed pure copper through equal channel angular pressing, Materials Research Express, 5 (7) (2018) 076504. https://doi.org/10.1088/2053-1591/aacf36

[26] M. Ebrahimi, M. H. Shaeri, C. Gode, H. Armoon, M. Shamsborhan, The synergistic effect of dilute alloying and nanostructuring of copper on the improvement of mechanical and tribological response, Composites Part B: Engineering, 164 (2019) 508-516. https://doi.org/10.1016/j.compositesb.2019.01.077

[27] M. Y. Alawadhi, S. Sabbaghianrad, Y. C. Wang, Y. Huang, T. G. Langdon, Characteristics of grain refinement in oxygen-free copper processed by equal-channel angular pressing and dynamic testing, Materials Science and Engineering: A, 775 (2020) 138985. https://doi.org/10.1016/j.msea.2020.138985[28] M. Rifai, and H. Miyamoto, Effect of strain energy on the grain growth behaviour of ultrafine-grained iron-chromium alloy by equal channel angular pressing, Journal of Mechanical Engineering and Sciences, 14 (3) (2020) 7049-7057. https://doi.org/10.15282/jmes.14.3.2020.07.0552

[29] M. Rifai, M. Yuasa, H. Miyamoto, Enhanced corrosion resistance of ultrafine-grained Fe-Cr alloys with subcritical Cr contents for passivity, Metals, 8 (3) (2018) 149. https://doi.org/10.3390/met8030149

[30] M. Rifai, H. Miyamoto, Effect of stored energy on corrosion fatigue properties of ultrafine grained Fe-20% Cr steel by equal channel angular pressing, IOP Conference Series: Materials Science and Engineering,

673 (1) (2019) 012131.
https://doi.org/10.1088/1757-899X/673/1/012131

[31] M. Rifai, M. Yuasa, H. Miyamoto, Effect of Deformation Structure and Annealing Temperature on Corrosion of Ultrafine-Grain Fe-Cr Alloy Prepared by Equal Channel Angular Pressing, International Journal of Corrosion, (2018) 4853175.
https://doi.org/10.1155/2018/4853175

[32] R, Nebojša Ž., Martina D. Gilić, I. Anzel, R. Rudolf, M. Mitrić, M.J. Romčević, B. B. Hadžić, Danijela Joksimović, M. Petrovic Damjanovic, M. Kos, Determination of microstructural changes by severely plastically deformed copper-aluminum alloy: Optical study, Journal of Mining and Metallurgy, Section B: Metallurgy, 50 (1) (2014) 61-68.
https://doi.org/10.2298/JMMB140121007R

UTICAJ NAPREZANJA NA KOROZIVNO PONAŠANJE ULTRA SITNOZRNOG BAKRA PRIPREMLJENOG INTENZIVNOM PLASTIČNOM DEFORMACIJOM

M. Rifai [a*], M. Mujamilah [b], E. Bagherpour [c], H. Miyamoto [d]

[a] Centar za istraživanje i tehnologiju naprednih nuklearnih materijala, Nacionalna agencija za istraživanje i inovacije, Serpong, Tangerang Selatan, Banten, Indonezija
[b] Istraživački centar za detekciju zračenja i nuklearnu analizu, Istraživačka organizacija za nuklearnu energiju, Nacionalna agencija za istraživanje i inovacije, Serpong, Tangerang Selatan, Banten, Indonezija
[c] Brunel centar zanaprednu tehnologiju očvršćavanja, Brunel univerzitet u Londonu London, Uksbridž, Ujedinjeno Kraljevstvo
[d] Odsek za mašinstvo, Došiša univerzitet, Kjotanabe, Kyoto, Japan

Apstrakt

Uticaj naprezanja na koroziono ponašanje ultra sitnozrnog (UFG) bakra pripremljenog intenzivnom plastičnom deformacijom (SPD) ispitan je u pogledu mikrostrukturne evolucije. SPD obrađeni materijal je pokazao ultra sitnozrnu (UFG) strukturu nakon prečišćavanja zrna tokom nekoliko vremenskih procesa, što će uticati na mehaničko i koroziono ponašanje. Homogenost se može efikasno postići kroz proces presovanja, jednostavne ekstruzije smicanja (SSE), koja je jedna od SPD tehnika. Čisti bakar je obrađivan SSE procesom tokom dva, četiri, osam i dvanaest prolaza. Struktura uzorka tretiranog SSE posmatrana je laserskim mikroskopom i transmisionim elektronskim mikroskopom, kao i difrakcijom rendgenskih zraka. Pomoću potenciodinamičke polarizacione krive primećeno je korozivno ponašanje u modifikovanom Livingstonovom rastvoru, 1 M NaCl i rastvoru sumpora. Struktura uzorka tretiranog SSE pokazala je da je prvi prolaz uzorka obrađenog SSE pokazao veliku deformaciju razvijanjem izdužene strukture zrna i podzrna. Povećanjem SSE broja prolaza, oblik zrna je postao jednakoosan zbog prevelikog naprezanja. Širenje rendgenskih zraka na uzorku bakra sa ultra sitnozrnastom strukturom (UFG) obrađenog SSE dovelo je do manje veličine kristalita, većeg mikronaprezanja i veće gustine dislokacije. Na materijalu sa UFG strukturom razvijen je homogeniji pasivni film. Međutim, gustina struje u 1 M NaCl je smanjena povećanjem broja prolaza usled rastvaranja metala bakra. UFG struktura ima više granica od grubo zrnaste strukture, a ovi fenomeni pokazuju zašto sposobnost rastvaranja Cu utiče na gustinu struje. Granica zrna se ponaša kao katodno mesto.

Ključne reči: *Plastična deformacija; Naprezanje; Ultra sitnozrna struktura; Granica zrna*